Available online at www.sciencedirect.com

ScienceDirect

Procedia IUTAM 15 (2015) 278 – 285

Procedia IUTAM

www.elsevier.com/locate/procedia

IUTAM Symposium on Multiphase flows with phase change: challenges and opportunities, Hyderabad, India (December 08 – December 11, 2014)

Lubricated Transport of Highly Viscous Non-Newtonian Fluid as Core-Annular Flow: A CFD Study

Sumit Tripathi[a], Amitabh Bhattacharya[b,*], Ramesh Singh[b], Rico F. Tabor[c]

[a]*IITB-Monash Research Academy, Mumbai, India*
[b]*Department of Mechanical Engineering, IIT Bombay, Mumbai, India*
[c]*School of Chemistry, Monash University, Australia*

Abstract

In this work, we investigate Core Annular Flow (CAF) using computational techniques for the case in which the core fluid is non-Newtonian and the annular fluid is Newtonian. The CAF is simulated using the CFD software ANSYS FLUENT 14.5 in a horizontal pipe. The core fluid is a highly viscous shear-thickening oil while water, the annular fluid, is injected along the thin annular region. Volume of fluid (VOF) modelling is used to simulate the immiscible liquid pair in the limit of low Reynolds number (*Re*). We analyse data related to the pressure drop along the pipe and the hydrodynamics of flow. Grid convergence analysis is performed before selecting a suitable mesh for simulation, and the effect of changing the interfacial tension between the oil and water phases is also studied. It is observed that the lower the interfacial tension, the more stable is the CAF. We also observe that, for lower interfacial tension, the pressure drop is reduced to a value close to that for a pure water flow–demonstrating that a highly viscous non-Newtonian fluid can be effectively transported using the CAF lubrication method. A theoretical analysis is also reported for a fully developed flow, in which both fluids are non-Newtonian. Good agreement is seen between the mean velocity profiles predicted by theory and simulation.

Peer-review under responsibility of Indian Institute of Technology, Hyderabad.

Keywords: Non-Newtonian fluid, core-annular flow, highly viscous oil

1. Introduction

Highly viscous oils and other complex fluids cannot be easily transported *via* pipelines by themselves due to the high pressure drop required to pump these materials. Several authors have suggested benefits of using Core-Annular Flows (CAFs), wherein the oil phase is in the center of the pipe and a lubricating layer of water flows adjacent to the wall surface[1,2,3,5,6,7]. In CAFs, pumping pressures are lower, since they are balanced by the lower wall-shear stresses acting on the annular fluid. In practice, however, perfect CAF is difficult to achieve, since waves are generated at the interface of the water and the oil, leading to Wavy Core Annular Flow (WCAF)[2,7,5]. Extensive literature is available

* Corresponding author. Tel.: +91-22-2576-7539
E-mail address: bhattach@iitb.ac.in

Peer-review under responsibility of Indian Institute of Technology, Hyderabad.
doi:10.1016/j.piutam.2015.04.038

on CAF, including models for levitation, stability studies, empirical studies of the energy efficiency of different flow types, empirical correlations providing information on the pressure drop *versus* mass flux *etc.*[2,7,5,6]. However, almost all of the studies to date have been performed with the assumption of a constant viscosity core fluid. CAFs have also been extensively studied through CFD with cases of sudden contraction, sudden expansion and return bends; however, even in these studies, the viscosity of the core fluid is considered to be constant[8,9,10]. The present work considers possible transportation of a highly viscous non-Newtonian fluid using CAF by employing CFD simulation. This paper starts with a theoretical study of flow equations for the two cases: (1) a power-law fluid lubricated with a Newtonian fluid and (2) when both the fluids are power law fluids with different consistency and flow-behavior indices. A simulation of CAF is then attempted using the software package ANSYS FLUENT 14.5, with a non-Newtonian (shear thickening) fluid as the core, and water as the annulus.

2. Flow equations

2.1. Power-law fluid lubricated with a Newtonian fluid

The case of axisymmetric CAF with two incompressible and immiscible fluids is considered, as shown in Figure 1. The core is a non-Newtonian (power law) fluid, while water flows in the annular region. The flow is assumed to be steady and fully developed, with zero radial and azimuthal velocity. The fluid velocity in the z direction is denoted by u_z, while η is the interface height. The relationships between shear stress and shear rate for core and annular fluids, respectively, are:

$$\tau_{rz}^{(1)} = \mu_1 \left(-\frac{du_z^{(1)}}{dr} \right)^n \quad \text{and} \quad \tau_{rz}^{(2)} = \mu_2 \left(-\frac{du_z^{(2)}}{dr} \right) \tag{1}$$

where μ_1 and n are the consistency and flow behavior indices of the core fluid, while μ_2 is the (Newtonian) viscosity of annular fluid, in this case, water.

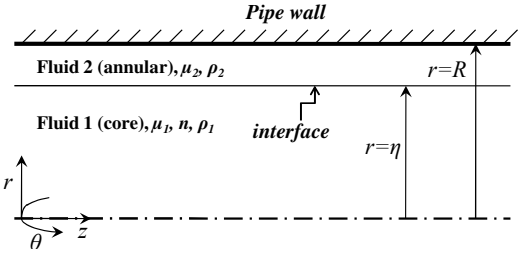

Fig. 1. Sketch of axisymmetric core-annular flow.

By applying a force balance approach to the core fluid and by using the Navier-Stokes equations for the annular fluid, the following differential equations can be obtained:

$$\frac{\mathrm{d}u_z^{(1)}}{\mathrm{d}r} = -\left(\frac{\chi}{2\mu_1} \right)^{1/n} r^{1/n} \quad \text{and} \quad \frac{\mathrm{d}u_z^{(2)}}{\mathrm{d}r} = -\frac{\chi r}{2\mu_2} + \frac{c}{r}, \tag{2}$$

where χ is the negative of the pressure gradient and c is a constant. The superscripts (1) and (2) represent the core and annular fluids, respectively. The boundary conditions for this flow system are:

$$\tau_{rz}^{(1)} = \tau_{rz}^{(2)} \ \text{ at } \ r = \eta, \qquad u_z^{(1)} = u_z^{(2)} \ \text{ at } \ r = \eta, \qquad u_z^{(2)} = 0 \ \text{ at } \ r = R. \tag{3}$$

The velocity profiles for the two fluids can be obtained by solving the differential equation (2) using the boundary conditions shown in equation (3) as:

$$u_z(r) = \begin{cases} \left(\frac{n}{n+1} \right) \left(\frac{\chi}{2\mu_1} \right)^{1/n} \left(\eta^{\frac{n+1}{n}} - r^{\frac{n+1}{n}} \right) + \frac{\chi}{4\mu_2} \left(R^2 - \eta^2 \right) & ; 0 \le r \le \eta \\ \frac{\chi}{4\mu_2} \left(R^2 - r^2 \right) & ; \eta \le r \le R \end{cases} \tag{4}$$

From this expression, the non-dimensional form of the velocity profiles can be obtained as:

$$u_z(r) = \begin{cases} 1 + \left(\frac{2n}{n+1}\right)\left(\frac{\chi R}{2}\right)^{\frac{1-n}{n}} \left(\frac{\mu_2}{\mu_1^{1/n}}\right)\left(\frac{\tilde{\eta}^{\frac{n+1}{n}} - \tilde{r}^{\frac{n+1}{n}}}{1-\tilde{\eta}^2}\right) & 0 \le \tilde{r} \le \tilde{\eta} \quad \text{;for core} \\ 1 + \left(\frac{\tilde{\eta}^2 - \tilde{r}^2}{1-\tilde{\eta}^2}\right) & \tilde{\eta} \le \tilde{r} \le 1 \quad \text{;for annular} \end{cases} \tag{5}$$

where $\tilde{\eta}$ and $\tilde{r}$ are non-dimensional parameters defined as: $\tilde{\eta} = \eta/R$ and $\tilde{r} = r/R$. From equation (4) The interface velocity (u_I, at $r = \eta$) can be observed as:

$$u_I = \frac{\chi}{4\mu_2}\left(R^2 - \eta^2\right) \tag{6}$$

The flow-rates for the two fluids are given by:

$$Q = \begin{cases} 2\pi \int_0^{\eta} r u_z^{(1)}(r) dr & \text{;for core} \\ 2\pi \int_{\eta}^{R} r u_z^{(2)}(r) dr & \text{;for annular} \end{cases} \tag{7}$$

This results in the following expressions for flow-rates and average velocities for the two fluids:

$$Q = \begin{cases} \frac{\pi n}{3n+1}\left(\frac{\chi}{2\mu_1}\right)^{1/n} \eta^{\frac{3n+1}{n}} + \frac{\pi\chi\eta^2}{4\mu_2}\left(R^2 - \eta^2\right) & \text{;for core} \\ \frac{\pi\chi}{8\mu_2}\left(R^2 - \eta^2\right)^2 & \text{;for annular} \end{cases} \tag{8}$$

$$U_{avg} = \begin{cases} \frac{n}{3n+1}\left(\frac{\chi}{2\mu_1}\right)^{1/n} \eta^{\frac{n+1}{n}} + \frac{\chi}{4\mu_2}\left(R^2 - \eta^2\right) & \text{;for core} \\ \frac{\chi}{8\mu_2}\left(R^2 - \eta^2\right) & \text{;for annular} \end{cases} \tag{9}$$

2.2. Both the fluids are power-law fluids

If both of the fluids (core and annular) are power-law fluids, the relationships between the shear stress and the shear rate can be written as:

$$\tau_{rz}^{(1)} = \mu_1\left(-\frac{du_z^{(1)}}{dr}\right)^{n_1} \quad \text{and} \quad \tau_{rz}^{(2)} = \mu_2\left(-\frac{du_z^{(2)}}{dr}\right)^{n_2} \tag{10}$$

where μ_i and n_i are the consistency and flow behavior indices. Here, i=1,2 represents Fluid 1 and Fluid 2, respectively. A few studies have been reported on the case in which both the fluids are power-law fluids but have the same flow-behavior indices ($n_1 = n_2 = m$)[11,12]. Here, a case is considered in which the two fluids have different flow-behavior indices.

By using a force balance approach for both the fluids and by using the boundary conditions shown in equation (3), the following velocity profiles can be obtained in a similar way:

$$u_z(r) = \begin{cases} 1 + \frac{n_1(n_2+1)}{n_2(n_1+1)}\left(\frac{\chi R}{2}\right)^{\frac{n_2-n_1}{n_1 n_2}} \left(\frac{\mu_2^{1/n_2}}{\mu_1^{1/n_1}}\right)\left(\frac{\tilde{\eta}^{\frac{n_1+1}{n_1}} - \tilde{r}^{\frac{n_1+1}{n_1}}}{1-\tilde{\eta}^{\frac{n_2+1}{n_2}}}\right) & 0 \le \tilde{r} \le \tilde{\eta} \\ 1 + \left(\frac{\tilde{\eta}^{\frac{n_2+1}{n_2}} - \tilde{r}^{\frac{n_2+1}{n_2}}}{1-\tilde{\eta}^{\frac{n_2+1}{n_2}}}\right) & \tilde{\eta} \le \tilde{r} \le 1 \end{cases} \tag{11}$$

In this case, the flow-rates and average velocities can be obtained as:

$$Q = \begin{cases} \frac{\pi n_2}{n_2+1}\left(\frac{\chi}{2\mu_2}\right)^{1/n_2}\left(R^{\frac{n_2+1}{n_2}} - \eta^{\frac{n_2+1}{n_2}}\right)\eta^2 + \frac{\pi n_1}{3n_1+1}\left(\frac{\chi}{2\mu_1}\right)^{1/n_1} \eta^{\frac{3n_1+1}{n_1}} & \text{; for core} \\ \frac{\pi}{N(N-2)}\left(\frac{\chi}{2\mu_2}\right)^{1/n_2}\left[NR^{N-2}(R^2 - \eta^2) - 2(R^N - \eta^N)\right] & \text{; for annular} \end{cases} \tag{12}$$

$$U_{avg} = \begin{cases} \frac{n_2}{n_2+1}\left(\frac{\chi}{2\mu_2}\right)^{1/n_2}\left(R^{\frac{n_2+1}{n_2}} - \eta^{\frac{n_2+1}{n_2}}\right) + \frac{n_1}{3n_1+1}\left(\frac{\chi}{2\mu_1}\right)^{1/n_1} \eta^{\frac{n_1+1}{n_1}} & \text{; for core} \\ \frac{1}{N(N-2)}\left(\frac{\chi}{2\mu_2}\right)^{1/n_2}\left[NR^{N-2} - 2\left(\frac{R^N - \eta^N}{R^2 - \eta^2}\right)\right] & \text{; for annular} \end{cases} \tag{13}$$

where $N = \frac{3n_2+1}{n_2}$. In the present paper, the study is carried out by simulating the CAF with a power-law fluid as the core and water (Newtonian fluid) as the annulus.

3. Model development

3.1. Model geometry and assumptions

A two-dimensional, axisymmetric transient model has been developed to study the horizontal CAF. The flow geometry is shown schematically in Figure 2(a) and a representational image of the model is shown in Figure 2(b) . A pipe of diameter 0.003 m and length 0.025 m has been considered for the analysis. A highly viscous non-Newtonian power law fluid with a consistency index (μ_1) = $10Pa \cdot s^n$ and a power law index (n)=1.2 is introduced as the core, while water ($\mu_2 = 1.003 \times 10^{-3} Pa \cdot s$) is injected through a nozzle into the annular space. The densities of the core and the annular fluids are $\rho_1 = 1100 kg/m^3$ and $\rho_2 = 998.2 kg/m^3$, respectively. Gravity has been ignored since we are studying an axisymmetric setup. The CFD software package ANSYS FLUENT 14.5 is used for the simulation[4]. The two fluids are assumed to be immiscible and incompressible. The case of low Reynolds number (Re) is studied to generate useful data regarding the pressure drop and hydrodynamics of flow. Since the two fluids share a relatively well-defined interface, the Eulerian-Eulerian based Volume of Fluid (VOF) model has been used. Mesh generation was completed after performing grid-sensitivity analysis.

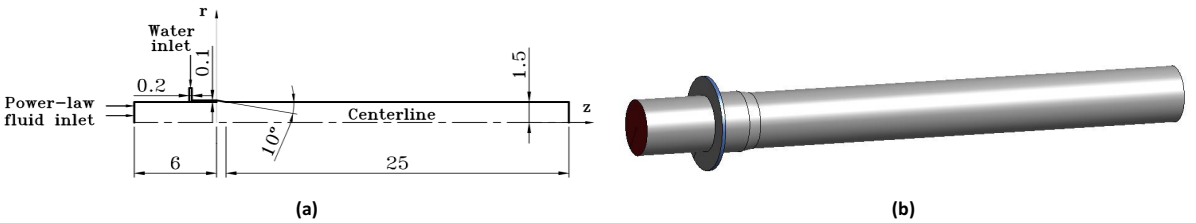

Fig. 2. (a) Model geometry (all dimensions are in milimeters) (b) Schematic representation of the CAF system.

3.2. Governing equations

The continuity and momentum conservation equations are solved by ANSYS FLUENT for all types of flows[4]. The continuity equation is given as:

$$\frac{\partial \rho}{\partial t} + \nabla . \left(\rho \vec{u} \right) = S_m \tag{14}$$

where $\rho, \vec{u}$ and S_m are the density, velocity-vector and mass-source terms, respectively. In the present analysis, S_m is zero. The VOF model solves a single set of momentum equations and tracks the volume fractions of each fluid throughout the domain[4]. The momemtum equation is given as:

$$\frac{\partial}{\partial t} \left(\rho \vec{u} \right) + \nabla . \left(\rho \vec{u} \, \vec{u} \right) = -\nabla p + \nabla . \left[\mu \left(\nabla \vec{u} + \nabla \vec{u}^T \right) \right] + \rho g + \vec{F} \tag{15}$$

where p, μ, g and $\vec{F}$ are the pressure in the flow-field, the viscosity, the gravitational acceleration and the body forces, respectively.

3.3. Volume of Fluid (VOF) model

The VOF model assumes that the two fluids are not inter-penetrating. For each additional phase, a new volume fraction variable is introduced in the computational domain. In each cell, the sum of volume fractions of all phases results in unity. The shared-fields approximation illustrates the sharing of variables and properties in any given cell by one or more fluids, depending on their volume fractions. Thus, if p^{th} fluid's volume fraction in the cell is represented as β_p, then the following three conditions are possible[4]:

- $\beta_p = 0$: the cell is empty (of the p^{th} fluid)

- $\beta_p = 1$: the cell is full (of the p^{th} fluid)
- $0 < \beta_p < 10$: the cell contains the interface between one or more other fluids

The interface between the phases is tracked by solving the continuity equation of the volume fraction of phases. For the p^{th} phase, this equation has the following form[4]:

$$\frac{1}{\rho_p}\left[\frac{\partial}{\partial t}\left(\beta_p \rho_p\right) + \nabla.\left(\beta_p \rho_p \overrightarrow{u}_p\right) = S_{\beta_p} + \sum_{q=1}^{n}\left(\dot{m_{qp}} - \dot{m_{pq}}\right)\right] \tag{16}$$

where $\dot{m_{qp}}$ is the mass transfer from the q_{th} phase to the p_{th} phase and $\dot{m_{pq}}$ is the mass transfer from the p_{th} phase to the q_{th} phase. For the primary phase, the volume fraction is computed by the following constraint and not by solving the volume fraction equation[4]:

$$\sum_{p=1}^{n} \beta_p = 1 \tag{17}$$

where n is the total number of phases. There are two immiscible fluids in the present study.

3.4. Boundary conditions and discretization

A two-dimensional, pressure-based, axisymmetric, transient solver is used with the VOF model. Water is specified as the primary phase and a power-law fluid as the secondary phase. The inlet and outlet boundary conditions are fixed as *velocity inlet* and *pressure outlet*, respectively. For all of the simulations, the core inlet velocity is kept as 0.03 m/s and that of water as 0.02 m/s. The center-line boundary condition is set as *axis* for the study of the axisymmetric case. A *no slip*, *no penetration* boundary condition is imposed at the wall. Initially, the domain is filled with only water. A schematic of the meshed geometry and the boundary conditions is shown in Figure 3.

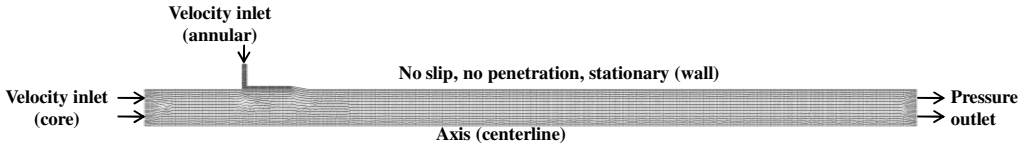

Fig. 3. Schematic of meshed geometry and boundary conditions.

A transient simulation with a fixed time step is performed to capture the dynamic behavior of the two-phase flow. Different methods are used for discretization of the governing equations. A first-order upwind method is used for the discretization of the momentum equation since this scheme provides a proper representation of the physics of flow. For pressure-velocity coupling, PISO (Pressure Implicit with Splitting of Operators) is used.

4. Results and discussions

4.1. Volume fraction contours

The contours of the volume fractions of the power-law fluid at different time values are shown in Figure 4(a) . A snapshot of the developed region is shown in Figure 4(b). In this case, the interfacial tension between the core and annular fluids is taken to be 0.02 N/m. A study in which interfacial tension is varied is performed later.

4.2. Pressure and velocity profiles

The variation of pressure in the axial direction and the streamwise velocity profiles in the fully developed region are shown in Figure 5(a) and (b), respectively. It can be seen that the pressure drop, even with the introduction of a

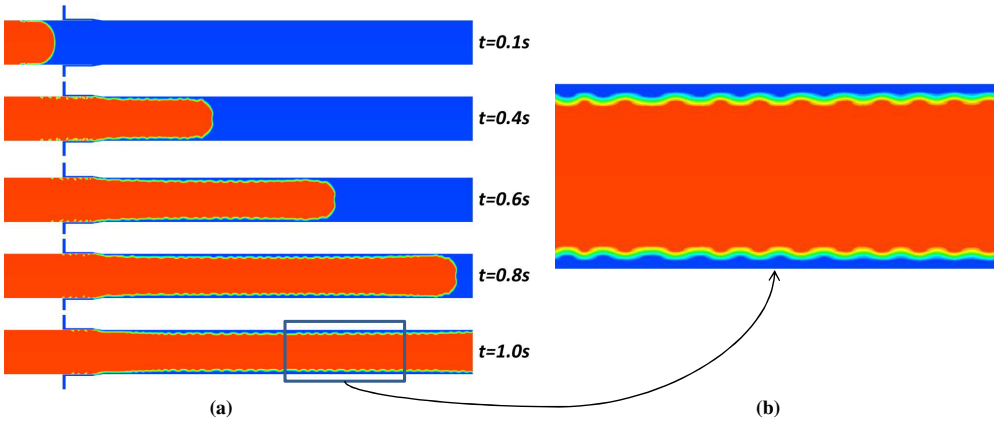

Fig. 4. Contours of water lubricated CAF with core fluid as power-law fluid, at different time values.

power-law fluid, remains almost the same as that in the case of only water. In the initial region, where only the core fluid is present, the pressure drop is considerably higher. The velocity profile shows that the flow of the highly viscous core fluid can be approximated as 'slug flow' with little deformation of the core. The velocity profiles are plotted in a developed domain shown in Figure 6(a). Figure 6(b) shows a comparison of the velocity profiles with theoretical and simulated results. The interface height (η) in equation (4) is calculated from Figure 4(b).

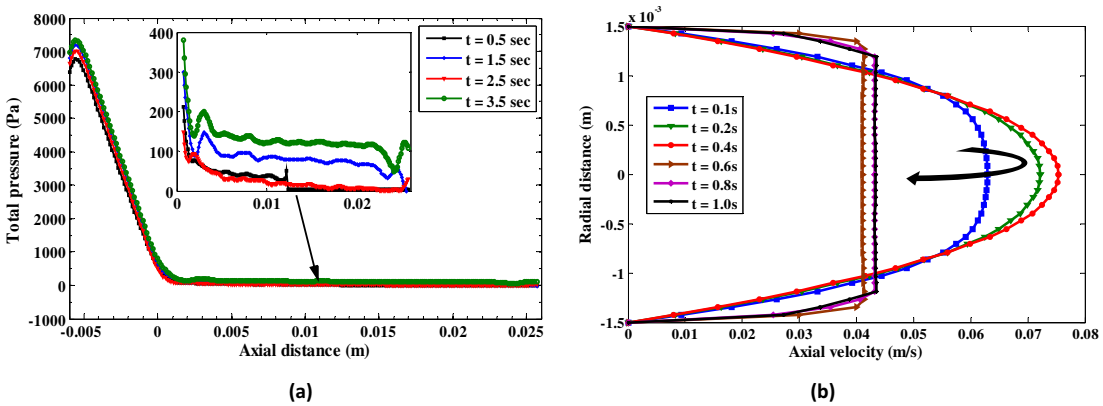

Fig. 5. (a) Axial pressure variations at different time values, (inset: CAF section) (b) Development of the CAF velocity profile.

4.3. Grid convergence analysis

Grid sensitivity (or grid independence) is investigated by comparing results from different levels of meshes. Typically, a grid convergence is said to be achieved when further changes in the solution are small enough to be neglected. In this study, three cases have been simulated, with different grid sizes, as shown in Table 1. Here, $\triangle z$ and $\triangle r$ are the grid resolutions in z (axial) and r (radial) directions, respectively. The total number of nodes in the geometry are typically refined by a factor of 1.5 with respect to the previous case. All other parameters (discretization methods, boundary conditions, time steps, *etc.*) in all three cases have been kept constant. The average streamwise velocity profile and the volume fraction are compared for different levels of mesh.

The results (at t=0.7 s) from the grid convergence study are shown in Figure 7. Figure 7(a) represents the axial-average of the volume fractions (ϕ_{avg}) of the core fluid in a specific domain, shown in Figure 6(a). Figure 7(b) represents the velocity profiles at different levels of mesh. The simulation is then carried out with the finest mesh among these three cases.

Table 1. Three cases of grid convergence studies with grid resolution in axial and radial directions, respectively

Cases	$\triangle z$ (μm)	$\triangle r$ (μm)
1	50	94
2	34	75
3	25	47

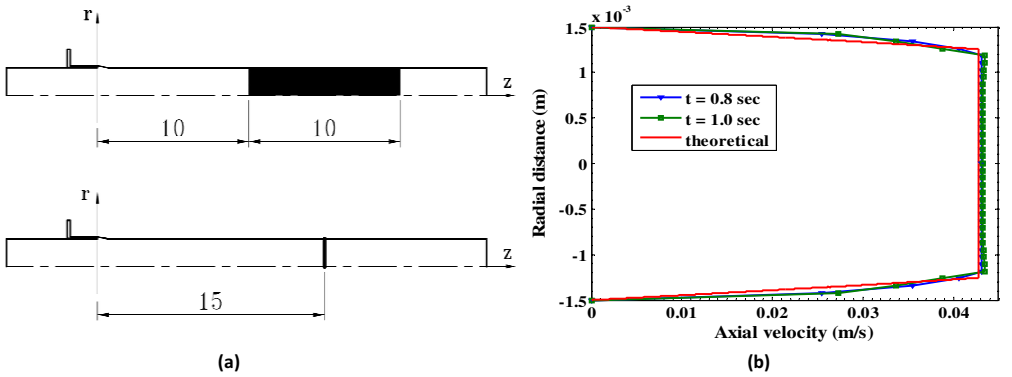

Fig. 6. (a) Sample domain in the developed region, (b) Comparison of theoretical and simulated velocity profiles (for theoretical profile: η = 1.256mm, χ = 255Pa/m).

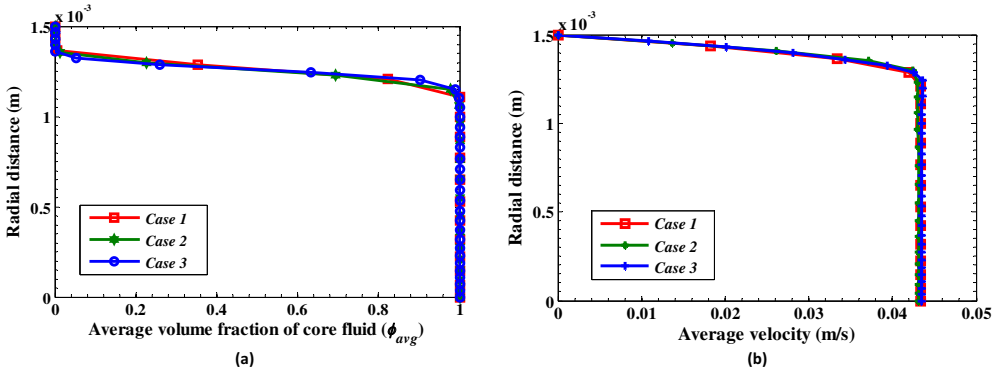

Fig. 7. Grid convergence results at different grid resolutions at t= 0.7s; (a) Radial variation of average volume fractions of the core fluid in the sample domain, (b) Velocity profiles in the sample domain.

4.4. Results: Effects of variation of interfacial tension

The effects of varying the interfacial tension (σ) between the two fluids on the CAF has been studied here for four different σ values: 0.01 N/m, 0.02 N/m, 0.03 N/m and 0.04 N/m. The results of this study are shown in Figure 8. It is observed that for the lowest value of the interfacial tension, the pressure drop is minimal. This is a direct result of the fact that at low values of interfacial tension, the interface is less wavy. At higher values of interfacial tension, the interface becomes more convoluted and fouling of the core is observed. This behavior is expected, since curved interfaces are energetically more favorable in higher surface tension. However, lowering the interfacial tension has its limitations; at ultra-low values of interfacial tension, emulsification may occur, in which the core fluid disperses into the annular fluid (or *vice versa*).

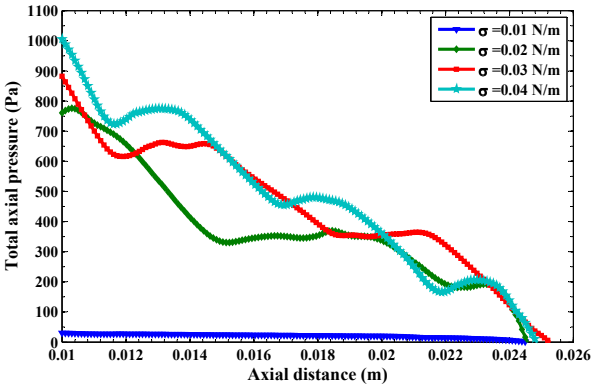

Fig. 8. Axial pressure variation for different interfacial tension values

5. Conclusions

Core-annular flow (CAF) is demonstrated to be a low-energy option for the pipe flow of highly viscous non-Newtonian fluids, with significantly lower pressure requirements than those required in pumping the viscous material natively. With CAF, the low viscosity of the annular fluid means that the pressure drop, and consequently the pumping power can be significantly reduced, with a concomitant reduction in energy cost. Simulations demonstrate that to achieve a stable CAF, the interfacial tension between the two fluids should, preferably, have a low value. Future development of these concepts will begin with a detailed study of interfacial instabilities, in order to understand the flow-behavior for a wide range of parameters and flow disturbances.

Acknowledgements

The authors are thankful to IITB-Monash Research Academy (India) and Orica Mining Services (Australia) for their support. The authors are also thankful to IIT Bombay for the licensed version of FLUENT 14.5.

References

1. Arney, M. S., Bai, R., Guevara, E., Joseph, D. D., Liu, K., Friction factor and holdup studies for lubricated pipeline-1. *International Journal of Multiphase Flow*, 1993; **1061-1076**: 19(No.6).
2. Bensakhria A, Peysson Y, Antonini G, Experimental Study of the Pipeline Lubrication for Heavy Oil Transport. *Oil & Gas Science and Technology - Rev. IFP* 2004; **523-533**: 59-5.
3. Chen, K, Bai, R., Joseph, D.D., Lubricated pipelining, Part 3. Stability of core-annular flow in vertical pipes. *J.Fluid Mech.*, 1990; **251-286**, 214.
4. Fluent 14.5 Users Guide, Fluent Inc., Lebanon, USA, 2012.
5. Ghosh S, Mandal T K, Das G, Das P K, Review of oil water core annular flow. *Renewable and Sustainable Energy Reviews* 2009 **1957-1965**: 13.
6. Hu H H, Lundgren T S, Joseph D D, Stability of core-annular flow with a small viscosity ratio. *Physics of Fluids A: Fluid Dynamics* 1990; **1945-1954**: 2(11).
7. Joseph D D, Bai R, Chan K P, Renardy Y Y, Core-Annular Flows. *Annu. Rev. Fluid Mech.* 1997; **65-90**:29.
8. Kaushik V.V.R., Sumana Ghosh, Gargi Das, Prasanta Kumar Das, CFD simulation of core annular flow through sudden contraction and expansion. *Journal of Petroleum Science and Engineering* 2012; **153-164**: 86-87.
9. Sumana Ghosh, Gargi Das, Prasanta Kumar Das, Simulation of core annular downflow through CFD-A comprehensive study. *Chemical Engineering and Processing: Process Intensification* 2010; **1222-1228**: 49.
10. Sumana Ghosh, Gargi Das, Prasanta Kumar Das, Simulation of core annular in return bendsA comprehensive CFD study. *Chemical engineering research and design* 2011; **2244-2253**: 89.
11. Sun Xue-Wei, Peng Jie, Zhu KeQin, Stability of core-annular flow of power-law fluids in the presence of interfacial surfactant. *Science China, Physics, Mechanics & Astronomy* 2010; **933-943**: 53.
12. Sun Xue-Wei, Peng Jie, Zhu Ke-Qin, The axisymmetric long-wave interfacial stability of core-annular flow of power-law fluid with surfactant. *Acta Mech. Sin.* 2012; **24-33**: 28(1).